GENETICS

pIGLET: Safe harbor landing sites for reproducible and efficient transgenesis in zebrafish

Robert L. Lalonde, Harrison H. Wells, Cassie L. Kemmler, Susan Nieuwenhuize, Raymundo Lerma, Alexa Burger, Christian Mosimann*

Standard zebrafish transgenesis involves random transgene integration with resource-intensive screening. While phiC31 integrase–based *attP*/*attB* recombination has streamlined transgenesis in mice and *Drosophila*, validated *attP*-based landing sites for universal applications are lacking in zebrafish. Here, we developed *phiC31 Integrase Genomic Loci Engineered for Transgenesis* (*pIGLET*) as transgenesis approach, with two *attP* landing sites *pIGLET14a* and *pIGLET24b* from well-validated Tol2 transgenes. Both sites facilitate diverse transgenesis applications including reporters and Cre/*loxP* transgenes. The *pIGLET14a* and *pIGLET24b* landing sites consistently yield 25 to 50% germline transmission, substantially reducing the resources needed for transgenic line generation. Transgenesis into these sites enables reproducible expression patterns in F0 zebrafish embryos for enhancer discovery and testing of gene regulatory variants. Together, our new landing sites streamline targeted, reproducible zebrafish transgenesis as a robust platform for various applications while minimizing the workload for generating transgenic lines.

INTRODUCTION

Transgenesis, the introduction of engineered DNA elements into the genome, is a key technique for any genetic model system. In zebrafish, transgenesis has resulted in invaluable fluorescent reporters and genetic modifier strains to study mechanisms of development, human disease, and physiology. However, routine transgenesis in zebrafish with random DNA integration via *Tol2* transposons or I-SceI meganuclease presents considerable challenges: The creation of high-quality, single-copy transgene integrations with reproducible activity remains time, labor, and resource intensive and faces unpredictable variability due to integration position effects that influence transgene activity (*1*–*8*). While CRISPR-Cas9–mediated knock-in has greatly advanced the possibilities to generate targeted transgene integrations, success rates remain locus dependent and variable (*9*–*11*). Transgenesis into well-validated "safe harbor" sites for reproducible, routine transgenesis into predictable loci remains a technical hurdle in zebrafish yet has the potential to positively transform the throughput, accessibility, and reproducibility of a key method in the model.

Adapted from the phiC31 bacteriophage, phiC31 integrase catalyzes the directional recombination of a vector-borne *attB* sequence into a genomic *attP* landing site that has been previously integrated by other transgenesis means (*12*–*15*). However, the identification of safe harbor sites in model organism genomes has remained conceptually and practically challenging due to the uncertain influences of genomic environment (position relative to genes, regulatory elements, repetitive sequences, open chromatin regions, etc.) on individual transgene integrations (*16*, *17*). Targeted vector integration using phiC31 integrase–mediated *attP*/*attB* recombination has transformed mouse and *Drosophila* transgenesis after well-defined, validated *attP* landing sites generated by random integration became accessible to the community (*18*–*21*). While phiC31 functions in zebrafish and has been applied for regulatory element testing with fluorescent reporters following *Tol2*-based random transgenesis of *attP* sites (*22*–*27*), universal *attP*-based landing sites that have been validated as potential safe harbors for a wide variety of transgene applications remain missing.

Here, converting two well-established *Tol2*-based transgenic integrations, we generated, validated, and applied two *attP* landing sites for key transgenesis applications using phiC31 integrase in zebrafish; we refer to this system as *phiC31 Integrase Genomic Loci Engineered for Transgenesis* (*pIGLET*). We demonstrate its utility in reproducibly generating high-quality zebrafish transgenics, including *loxP*-based reporters that are overly sensitive to position effects. Accessible with standard methods applied in the field, our two new landing sites enable qualitative and quantitative transgene applications, facilitate reproducible reagent generation and sharing, as well as streamline the transgenesis workflow while reducing required effort and animal numbers. Beyond two widely applicable landing sites for community use, our work proposes that conversion of high-quality *Tol2* transgenes into *attP* landing sites has the potential to drastically increase the number of transgenesis landing sites available in the field.

RESULTS

Converting two functional *loxP* transgenes into *attP* landing sites

Because of random integration, transgenes generated with the *Tol2* transposon system or I-SceI (fluorescent reporters, CreERT2 drivers, *UAS* effectors, etc.) are susceptible to position effects, requiring labor- and resource-intensive screening to identify transgenic founders with accurate, reproducible expression (*1*, *4*). A key tool for genetic lineage labeling, *loxP*-based reporter transgenes that recombine upon Cre recombinase activity, is also notably susceptible to position effects in zebrafish and challenging to generate (*4*). As they retain access for Cre recombinase action, we reasoned that well-recombining and well-expressing *loxP* reporter transgenes present suitable integration sites for transgenesis. We previously generated and characterized the *loxP*-based Cre reporter strains *ubi:loxP-EGFP-loxP_mCherry* (*ubi:Switch*) and *hsp70l:loxP-STOP-loxP_EGFP* (*hsp70l:Switch*) as *Tol2* transgene integrations with efficient

University of Colorado School of Medicine, Anschutz Medical Campus, Department of Pediatrics, Section of Developmental Biology, 12801 E 17th Avenue, Aurora, CO 80045, USA.
*Corresponding author. Email: christian.mosimann@cuanschutz.edu

recombination and expression (*17*, *28*, *29*). Both lines (i) have been in use for generations in numerous labs, (ii) feature dependable, reproducible *loxP* recombination upon Cre activity, and (iii) are homozygous viable without appreciable phenotypic consequences. We therefore performed CRISPR-Cas9–based knock-in of phiC31-recognized *attP* landing sites to replace the *Tol2* transgenes in these strains to generate alleles entitled *pIGLET* (fig. S1).

Our previous mapping of the genomic locations of both *ubi:Switch* and *hsp70l:Switch* had revealed that both had integrated into repetitive sequences (*17*), barring us from designing locus-specific CRISPR-Cas9 targeting strategies. We therefore devised a two-step process to generate *attP* landing sites in each locus that is applicable to any previously generated *Tol2* transgene (fig. S1): *Tol2*-based transgenes are flanked by unique 5′ and 3′ *Tol2* repeats, which we targeted using individual single guide RNAs (sgRNAs) for Cas9 ribonucleoprotein (RNP)–mediated transgene excision in homozygous transgenic embryos (fig. S1A). Screening for transgene-negative F1 embryos for both lines (see Materials and Methods), we identified clean deletions of the integrated transgenes (1/20 F0-injected embryos) that left a unique 5′-3′ *Tol2* repeat remnant sequence in the genome (step 1) (fig. S1, A to C, F, and G). We then targeted this sequence in embryos from heterozygous in-crosses using a single sgRNA and coinjected a single-stranded oligonucleotide (ssODN) containing an 84-bp-spanning *attP* sequence flanked by asymmetric homology arms of the remnant *Tol2* repeats (fig. S1D; see Materials and Methods for details). We identified near-complete *attP* integrations in both the *ubi:Switch* (1/18 F0-injected embryos) and *hsp70l:Switch* (1/35 F0-injected embryos) and designated these new alleles *pIGLET14a* (81-bp *attP*) and *pIGLET24b* (80-bp *attP*), respectively (step 2) (fig. S1, E, H, and I). Both *attP* integrations are homozygous viable and detectable with simple polymerase chain reaction (PCR) genotyping for line maintenance (see Materials and Methods).

To standardize nomenclature, we propose to name *pIGLET* landing sites with chromosome number and a consecutive letter index: *pIGLET14a*^{co2001} and *pIGLET24b*^{co2002}. We further propose to refer to transgene insertions into individual landing sites as *Tg(pIGLET14a.transgene)* or *Tg(pIGLET24b.transgene)*, shortened as *p14a.transgene* and *p24b.transgene* to distinguish loci in the text (e.g., *p14a.drl:EGFP* and *p24b.drl:EGFP*).

pIGLET14a and *pIGLET24b* are highly efficient landing sites

We next sought to test the *pIGLET14a* and *pIGLET24b* landing sites for phiC31 integrase–mediated transgenesis. A typical workflow to implement the *pIGLET* system for zebrafish transgenesis is described in Fig. 1 (A and B), including a schematic depicting targeted transgene integration into the landing sites and validation by PCR and sequencing. PCR-based genotyping of *attP*/*attB* recombination in *pIGLET14a* and *pIGLET24b* landing sites for quality control and validation of phiC31 *integrase* mRNA can be performed in stable transgenic lines and F0-injected embryos, with documented recombination within the first 24 hours postfertilization (hpf) in 100% of injected embryos with observable transgene expression (see Supplementary Methods). This simple quality control step provides confidence in the methods and reagents used, in a manner comparable to the now universal F0 testing of sgRNA functionality for CRISPR-Cas9 mutagenesis (*30*). One important distinction of phiC31 integrase–mediated transgenesis is that the entire *attB*-containing plasmid will be integrated into the *pIGLET* landing sites, while *Tol2* integrations only span the transposon without backbone. In addition to our previously established *attB*-containing *pDEST* backbone vectors (*pCM268*, no transgenesis marker; *pCM327*, *cryaa:Venus*) (*22*), we generated six additional backbone vectors for different cloning approaches: *pRL055 pDESTattB_cryaa:Venus* (inverted), *pRL56 pDESTattB_exorh:EGFP*, *pCK122 pDESTattB_exorh:mCherry*, *pCK123 pDESTattB_exorh:mCerulean*, *pRL092 pattB_cryaa:Venus_MCS*, and *pRL093 pattB_exorh:EGFP_MCS* (for details, see Table 1 and Materials and Methods). While *cryaa:Venus* provides an eye lens–specific transgenesis marker, the *exorh* element provides pineal gland-specific reporter expression for simple transgene screening (Table 1) (*31*). The *attB* site–containing *pDEST* vectors *pCM268*, *pRL055*, *pRL056*, *pCK122*, and *pCK123* are designed as backbones to generate expression plasmids using the Multisite Gateway system in combination with *p5E*, *pME*, and *p3E* plasmids (*2*, *31*). Alternatively, the *attB* site vectors *pRL092* and *pRL093* enable restriction enzyme- or PCR-based cloning and contain a multiple cloning site (MCS) with eight available unique restriction sites (NsiI, EcoRV, NheI, NdeI, SacI, BstEII, StuI, and AgeI) (Table 1). All vector maps and details of genomic locations of the landing sites are documented in the data file S1.

Using phiC31 integrase–mediated transgenesis, we next sought to integrate different *attB*-based transgenic reporter and effector vectors into *pIGLET14a* and *pIGLET24b* (tables S1 and S2). Accessible with standard methods applied in the field, phiC31 integrase–mediated transgenesis is performed by coinjection of an *attB* sequence–containing transgenesis vector together with mRNA encoding for the phiC31 integrase into one-cell stage zebrafish embryos, at comparable concentrations to those used in Tol2-mediated transgenesis [e.g., vector (25 ng/μl) and *integrase* mRNA (25 ng/μl)]. A key difference to other transgenesis approaches is the need to inject into zebrafish that carry an *attP* landing site, such as *pIGLET14a* and *pIGLET24b.* Consequently, we recommend injection into homozygous landing site embryos to provide optimal transgenesis efficiency. In the subsequent paragraphs, newly created transgenic lines will have *p14a* and *p24b* designations to reflect their *pIGLET* integration locus (e.g., *p14a.drl:EGFP* and *p24b.drl:EGFP*). Transgene integration in the *pIGLET14a* and *pIGLET24b* loci is highly efficient, routinely achieving 25 to 50% germline transmission from F0-injected zebrafish. A complete record of germline screening statistics for all lines recovered in the *pIGLET14a* and *pIGLET24b* loci is compiled in table S2. Unless specifically noted, all images depicted are of single-copy F2 heterozygous transgenic zebrafish. All F1, F2, and F3 transgenic zebrafish with expected targeted integration show consistent and uniform expression, with no evidence of generational silencing (fig. S8).

Tol2-based fluorescent reporters harnessing the 6.35-kb *drl* regulatory elements mark the emerging lateral plate mesoderm (LPM) and subsequently refine to cardiovascular and hematopoietic lineages (Fig. 1, E and F, and figs. S2, A and B, and S3, A and B) (*32*–*34*). To rederive *drl*-based reporters in each *pIGLET* landing site, we recloned the well-established reporter *drl:EGFP* into an *attB* site–carrying vector backbone and injected with phiC31 integrase–encoding mRNA into heterozygous in-crossed *pIGLET14a* and *pIGLET24b* offspring. Subsequent screening of potential founders resulted in more than 50% of injected zebrafish with germline-transmitting *drl:EGFP* in the corresponding landing site (table S2). For both landing sites, the resulting expression pattern and dynamics were comparable to the *Tol2*-based, *drl:mCherry* reporter

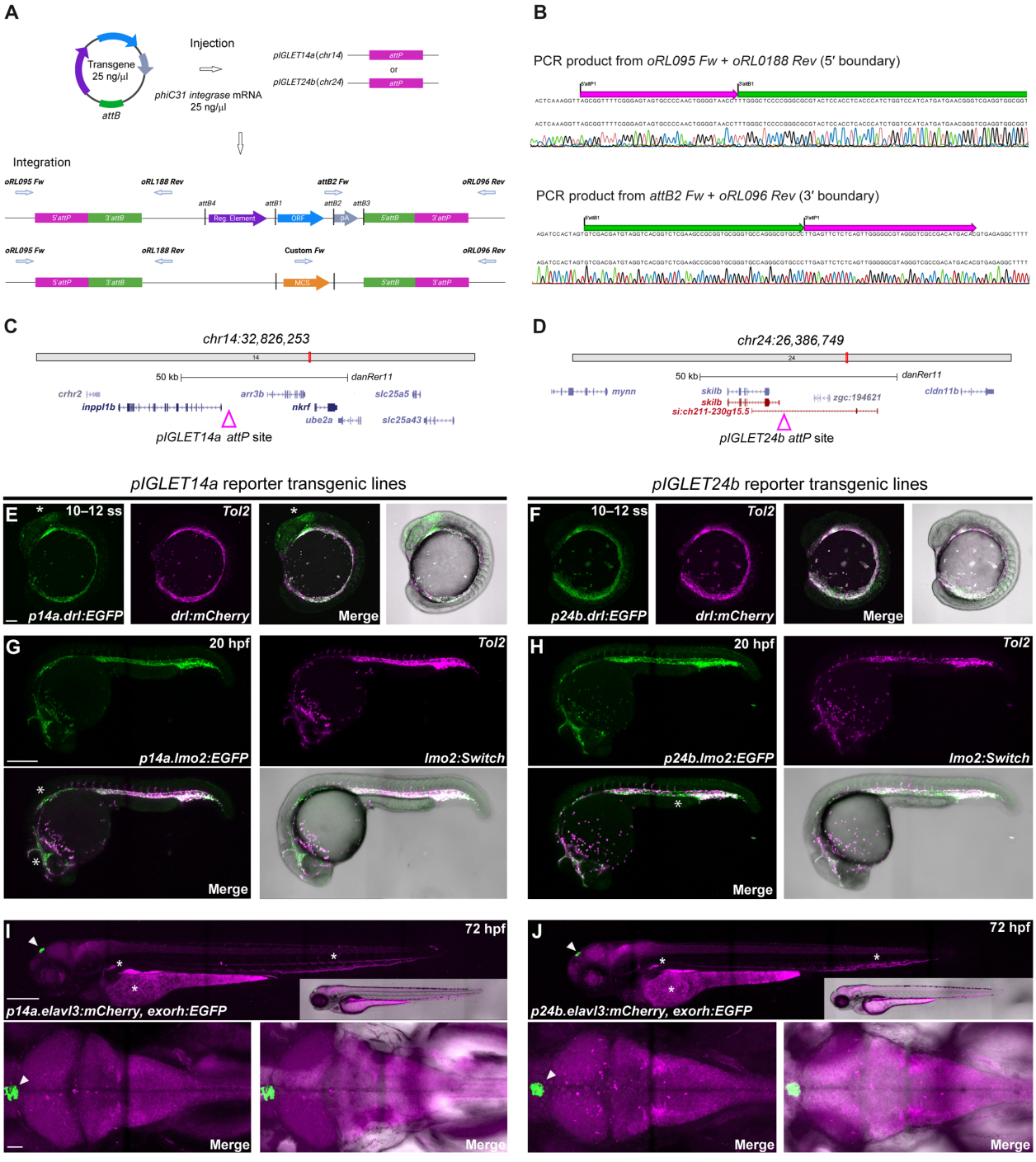

Fig. 1. Zebrafish *pIGLET14a* and *pIGLET24b* landing sites enable high-quality transgenics. (**A** and **B**) Schematic of *pIGLET* system workflow. Transgenes with *attB*-containing *pDEST* or MCS backbones are coinjected with phiC31 *integrase* mRNA into *pIGLET14a* or *pIGLET24b* zebrafish (A). Integration is depicted with both *attB*-containing *pDEST* (*pCM268*, *pRL055*, *pRL056*, *pCK122*, and *pCK123*) (top) or MCS (*pRL092* and *pRL093*) (bottom) backbones (A). The 5′ and 3′ transgene integration boundaries can be confirmed via PCR and sequencing (B). (**C** and **D**) Genomic locations of both landing sites. (**E** to **J**) Validating *pIGLET14a* and *pIGLET24b* with F2 *drl:EGFP, lmo2:EGFP,cryaa:Venus* and *elavl3:mCherry,exorh:EGFP*. (E and F) Crossed to *Tol2*-based *drl:mCherry*, *p14a.drl:EGFP* and *p24b.drl:EGFP* show analogous reporter activity in lateral plate mesoderm (LPM; 10 to 12 ss green fluorescence). Note faint brain expression in *p14a.drl:EGFP* (E, white asterisk) common with *Tol2*-based *drl* reporter transgenics with strong expression. (G and H) Crossed to *Tol2*-based *lmo2:Switch* (dsRed2, magenta), *p14a.lmo2:EGFP* and *p24b.lmo2:EGFP* show analogous, overlapping activity in endothelium at 20 hpf. *EGFP* expression is more consistent/complete compared to *dsRED2* in Tol2-based *lmo2:Switch* (G and H, white asterisk). (I and J) *p14a.elavl3:mCherry* and *p24b.elavl3:mCherry* show complete, consistent reporter expression in the central nervous system at 72 hpf, akin to previous Tol2-based *elavl3* transgenics. The *in cis exorh:EGFP* transgenesis marker indicated with white arrowhead. Note common autofluorescence in blood, kidney, and yolk (I and J, white asterisk). F2 heterozygous embryos are depicted (E to J). Scale bars: 100 µm (E), 250 µm (G), 250 µm (I), and 50 µm.

Table 1. *pIGLET* reagents. Table of landing site information, *pDEST* plasmids, and primers for *pIGLET* system implementation. See also data file S1 for vector maps and genomic loci (GenBank format).

Landing site location	Landing site name	Description
chr14:32,750,643	*pIGLET14a*	*attP* landing site, formerly *ubi:Switch* transgene
chr24:26,325,591	*pIGLET24b*	*attP* landing site, formerly *hsp70l:Switch* transgene
Plasmid ID	**Plasmid name**	**Description**
	Destination vectors *(pDEST*, *AmpR*, *CmlR*, and *ccdB)*	
pCM268	*pDESTattB* (no Tg marker)	Previously published (*22*)
pRL055	*pDESTattB_cryaa:Venus*	*cryaa:Venus-SV40pA* transgenesis marker
pRL056	*pDESTattB_exorh:EGFP*	*exorh:EGFP-SV40pA* transgenesis marker
pCK122	*pDESTattB_exorh:mCherry*	*exorh:mCherry-SV40pA* transgenesis marker
pCK123	*pDESTattB_exorh:mCerulean*	*exorh:mCerulean-SV40pA* transgenesis marker
	MCS backbone vectors (AmpR)	
pRL092	*pattB_cryaa:Venus_MCS*	*cryaa:Venus-SV40pA* transgenesis marker, multiple cloning site (NsiI, EcoRV, NheI, NdeI, SacI, BstEII, StuI, and AgeI)
pRL093	*pattB_exorh:EGFP_MCS*	*exorh:EGFP-SV40pA* transgenesis marker, multiple cloning site (NsiI, EcoRV, NheI, NdeI, SacI, BstEII, StuI, and AgeI)
Primer ID	**Primer name**	**Description**
oRL095	*Tol2 remnant Fw*	For landing site detection, *pIGLET14a* or *pIGLET24b* *5′-ATTGCCAGAGGTGTAAAGTA-3′*
oRL096	*Tol2 remnant Rev*	For landing site detection, *pIGLET14a* or *pIGLET24b* *5′-CCAGTACACGCTACTCAAA-3′*
oRL168	*ubi:Switch locus Fw*	*pIGLET14a* genotyping *5′-CATGATCGAAAACGAGCAATGTC-3′*
oRL169	*ubi:Switch locus Rev*	*pIGLET14a* genotyping *5′-GACTGCGTCACTTTGACAACCCTG-3′*
oRL074	*hsp70l:Switch locus Fw*	*pIGLET24b* genotyping *5′-GCATGACACGGCTAACCAAC-3′*
oRL073	*hsp70l:Switch locus Rev*	*pIGLET24b* genotyping *5′-TATCAGCACACACCTTTATCGC-3′*
oRL188	*5′ expression plasmid Rev*	5′ transgene integration check (with *oRL095*) *5′-GCCTTTGAGTGAGCTGATACC-3′*
attB2 Fw	*attB2 Fw*	3′ transgene integration check (with *oRL096*) *5′-ACCCAGCTTTCTTGTACAAAGTGG-3′*

transgenic line that was previously selected for faithful expression identical to *Tol2*-based *drl:EGFP* integrations (Fig. 1, E and F, figs. S2, A and B, and S3, A and B) (*33*). *p14a.drl:EGFP* shows faint brain expression (Fig. 1E) common with *Tol2*-based *drl* reporter transgenics with strong expression (*32*).

The regulatory elements of *lmo2* mark emerging endothelial and hematopoietic cell types (Fig. 1, G and H, and fig. S2, C and D) (*35*); however, *lmo2*-based fluorescent reporter constructs are highly susceptible to position effects, requiring screening of several independent random insertions to isolate faithful reporter activity (*35*, *36*). Germline-transmitted integrations of *p14a.lmo2:EGFP* and *p24b.lmo2:EGFP* showed labeling of vasculature and blood and more uniform expression compared to the previously described, *Tol2*-based *lmo2:Switch* transgenic line (*lmo2:loxP-dsRED2-loxP_EGFP*) (Fig. 1, G and H, and fig. S2, C and D) (*36*).

To investigate landing site functionality for nonmesodermal lineages, we created transgenic reporter lines based on the regulatory elements of *elavl3* (*HuC*), a pan-neuronal marker (*37*). Using the previously described 8.7-kb regulatory region (*38*, *39*), we created *elavl3:mCherry*,*exorh:EGFP* transgenic lines in both the *pIGLET14a* and *pIGLET24b* loci. *p14a.elavl3:mCherry* and *p24b.elavl3:mCherry* transgenes show expression in the brain and spinal cord comparable to previously described transgenic lines (Fig. 1, I and J) (*38*, *39*).

Examination of adult zebrafish confirmed that expression of transgenesis markers *cryaa:Venus* and *exorh:EGFP* are maintained throughout development in both *pIGLET14a* and *pIGLET24b* landing

sites (fig. S4, A to D). PCR-based genotyping of the recombined *attP*/*attB* sites confirmed precise transgene integrations of all characterized strains (see Supplementary Methods, Fig. 1B, and table S2). Together, these results underline the safe harbor potential of *pIGLET14a* and *pIGLET24b* for reproducible, high-quality transgenesis of fluorescent reporters with complex developmental expression patterns.

pIGLET14a and *pIGLET24b* allow predictable generation of Cre/*lox* transgenes

To test whether our landing sites are suitable to generate functional CreERT2 driver transgenes, we created *drl:creERT2* transgenic lines in both the *pIGLET14a* and *pIGLET24b* loci and compared their activity to the well-characterized *Tol2*-based *drl:creERT2* transgene (*32*, *40*–*43*). CreERT2 driver transgenes are also highly sensitive to position effects, with the highly efficient, *Tol2*-based *drl:creERT2* transgenic line requiring screening of 10 independent founders (*32*). By performing Cre/*loxP* lineage trace experiments with *hsp70l:Switch*, we compared the dynamics of the *drl* regulatory element in resolving complex LPM-based lineages (Fig. 2A). As previously described, shield stage 4-hydroxytamoxifen (4-OHT) induction using *Tol2*-based *drl:creERT2* results in complete LPM lineage labeling (heart, pectoral fin, endothelial cells, blood, kidney, and pharyngeal arch musculature) and a subset of paraxial lineage labeling (skeletal muscle and median fin fibroblasts) (Fig. 2A). A 4-OHT induction series demonstrates that by 12 ss (somite stage), only LPM lineages are labeled using *drl:creERT2*, albeit with notable mosaicism (Fig. 2A). This dynamic, induction time point–dependent lineage labeling is recapitulated in the newly generated *p14a.drl:creERT2* and *p24b.drl:creERT2* lines in the *pIGLET14a* and *pIGLET24b* loci (Fig. 2B and fig. S5A). Consistent with *p14a.drl:EGFP*, *p24b.drl:creERT2* shows faint brain tracing when induced with 4-OHT at shield stage. Notably, *pIGLET* landing sites now enable integration of CreERT2, Gal4 drivers, and other effector transgenes at the same locus as their reporter transgene counterpart, providing confidence in the activity of the regulatory elements across transgene types.

We next sought to test whether *loxP*-based reporters for Cre activity (so-called *Switch* lines) are functional in our new landing sites. *loxP*-based *Switch* reporters have a high sensitivity to position effects and are therefore challenging to generate using random integrations,

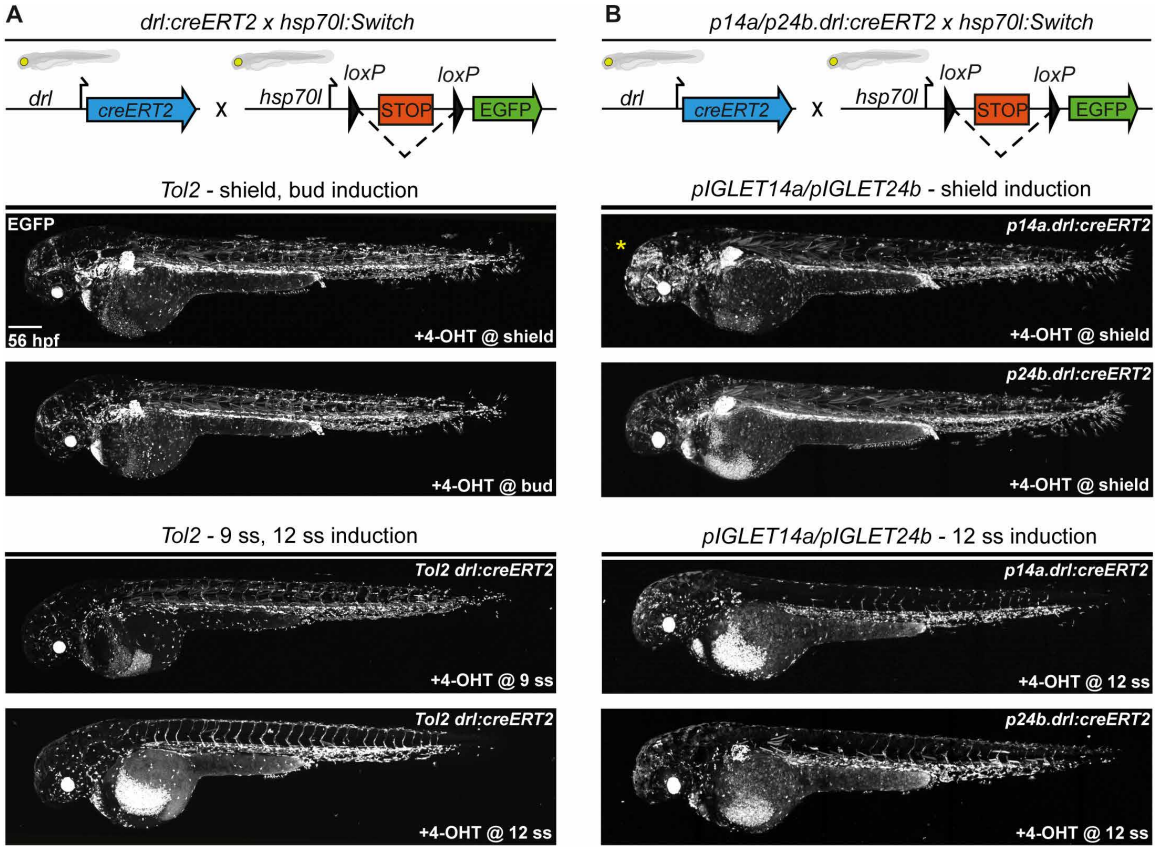

Fig. 2. CreERT2 driver transgenes have predictable and consistent activity in *pIGLET14a* and *pIGLET24b*. Comparison of CreERT2-mediated recombination of *Tol2*-based *drl:creERT2* and *pIGLET*-based lines *p14a.drl:creERT2* and *p24b.drl:creERT2* by crossing to the *loxP* reporter *hsp70l:Switch* and performing a 4-OHT induction series. Transgene and crossing schematics on top, lateral confocal views and anterior to the left. (**A** and **B**) Compared to the *Tol2*-based *drl:creERT2* transgenic line, *p14a.drl:creERT2* and *p24b.drl:creERT2* show accurate lineage contribution dynamics at 56 hpf when treated with 4-OHT at shield stage and 12 ss (A and B). Note that with shield stage 4-OHT induction, *drl*-expressing cells contributed both to the LPM lineages (heart, pectoral fin, endothelial cells, kidney, mesothelia, blood, pharyngeal arch musculature, and macrophages) and a subset of paraxial mesoderm lineages (median fin fibroblasts and skeletal muscle). With 12 ss 4-OHT induction, LPM lineages are specifically traced with more mosaic labeling of heart, pectoral fin, and kidneys (A and B). Consistent with our *p14a.drl:EGFP* reporter lines, some neuronal lineage labeling is observed with *p14a.drl:creERT2* when induced with 4-OHT at shield stage (yellow asterisk) (B). F2 heterozygous embryos are depicted (B). Scale bar, 200 μm.

requiring resource-intensive screening efforts to isolate well-recombining *Switch* transgene integrations (*1*, *4*, *17*, *28*, *29*, *44*–*47*). As the original *ubi:Switch* and *hsp70l:Switch* have high *loxP* recombination efficiency, we introduced a new *Switch* transgene termed *hsp70l:Switch2* (*hsp70l:loxP-STOP-loxP_mApple,cryaa:Venus*) that recombines from no fluorophore to mApple (red fluorescent), into each the two new *pIGLET* loci.

We tested the recombination efficiency of *hsp70l:Switch2* in both *pIGLET14a* and *pIGLET24b* with several previously published CreERT2-driver lines: *ubi:creERT2* (*29*), *drl:creERT2* (*32*), and *crestin:creERT2* (*48*), each induced with 4-OHT and imaged at 56 hpf (Fig. 3, A and B). When crossed to *ubi:creERT2* and *drl:creERT2*, *hsp70l:Switch2* displayed high levels of recombination and reporter expression upon heat shock akin to the previously described *hsp70l:Switch* (Figs. 2A and 3, A and B) (*17*, *28*, *49*, *50*). *crestin* is expressed in early neural crest cells during early somitogenesis and becomes undetectable by 72 hpf, with *crestin:creERT2* enabling mosaic lineage labeling of neural crest cells throughout development, instrumental for lineage studies and tracking of melanoma tumors (*48*, *51*–*53*). Consistent with *hsp70l:Switch*-based lineage labeling (fig. S5D) and previous observations using *ubi:Switch* (*48*), we crossed *hsp70l:Switch2* to *crestin:creERT2* and observed mosaic recombination in neural crest cells (Fig. 3, A and B, and fig. S5, B and C). Together, our benchmarking establishes that *loxP*-based Switch reporters show faithful expression and sensitive, reproducible Cre-mediated recombination when integrated into the *pIGLET14a* and *pIGLET24b* landing sites. This property facilitates the predictable, efficient generation of new Cre-responsive *Switch* reporters and effector lines in zebrafish, overcoming a critical technical bottleneck in the field.

As previously documented for vector injection–based transgenesis in zebrafish by any method (*1*, *22*, *26*), approximately 8 to 10% of germline-transmitted events result from random background integration caused by transgene vector that linearized at different locations in its sequence. We also uncovered such events using *pIGLET*-targeted phiC31 integrase–mediated transgenesis based on lower or variable transgene expression among reporter-expressing embryos (6 of 76 clutches analyzed, 7.89%) (table S2). These events predominantly occurred with plasmid sizes of ~14 kb or greater (five of six nontargeted integration clutches) (table S2). A limitation with this system as compared to *Tol2*-based injections is that the entire plasmid integrates at the landing site, increasing overall transgene sizes. To decrease overall plasmid size, injection of a minicircle

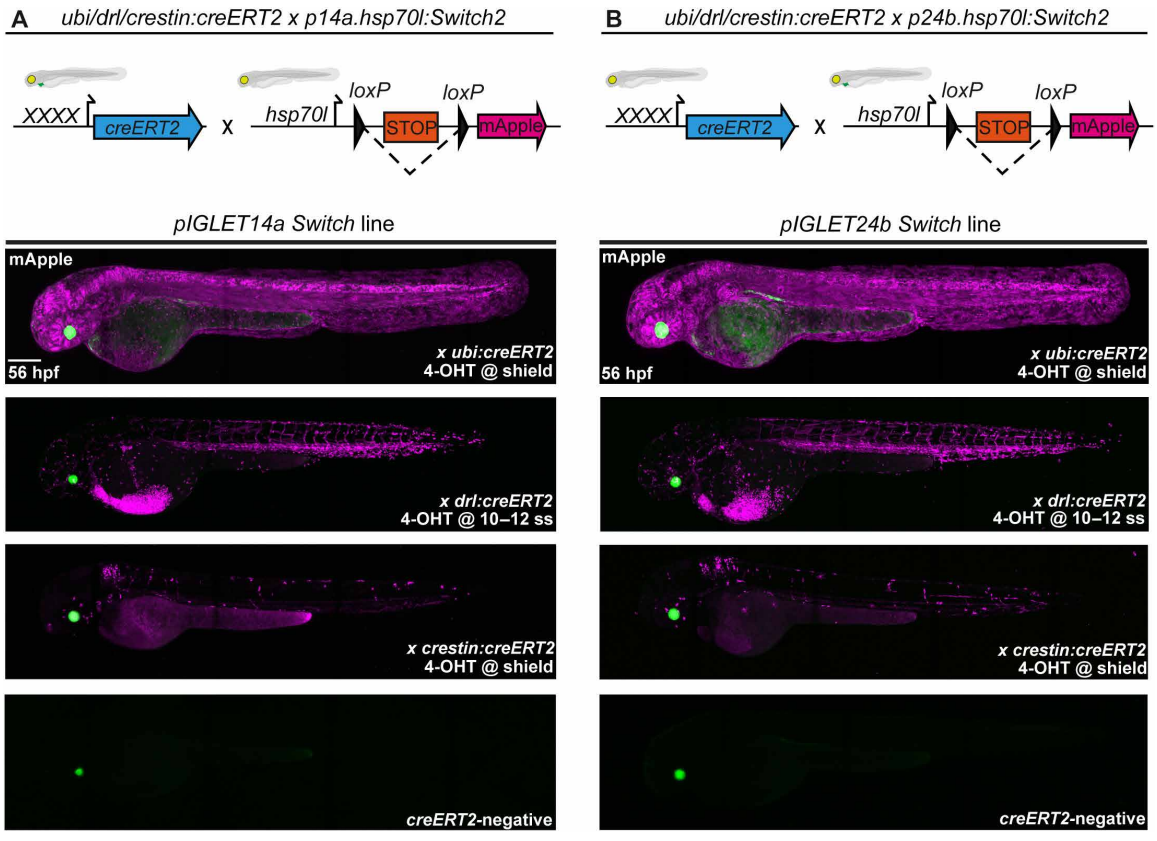

Fig. 3. *loxP Switch* transgenes have predictable and consistent activity in *pIGLET14a* and *pIGLET24b*. Comparison of CreERT2-mediated recombination of *pIGLET*-based *loxP* reporter *hsp70l:Switch2*. Transgene and crossing schematics on top, lateral confocal views and anterior to the left. (**A** and **B**) Testing of *p14a.hsp70l:Switch2* and *p24b.hsp70l:Switch2* with three independent CreERT2-driver lines: *ubi:creERT2*, *drl:creERT2*, and *crestin:creERT2*. *p14a.hsp70l:Switch2* and *p24b.hsp70l:Switch2* drive strong *mApple* reporter expression following CreERT2-mediated recombination when crossed to ubiquitous and tissue-specific CreERT2-driver lines, treated with 4-OHT, and imaged at 56 hpf (A and B). Note the near-complete *mApple* labeling of the embryo at 56 hpf when *p14a.hsp70l:Switch2* and *p24b.hsp70l:Switch2* are combined with *ubi:creERT2* and accurate labeling of the LPM or neural crest cells when used in combination with *drl:creERT2* or *crestin:creERT2*, respectively, akin to previous results using *Tol2*-based versions of either CreERT2 driver (A and B). F2 heterozygous embryos are depicted (A and B). Scale bar, 200 μm.

plasmid could be performed as routinely used mouse transgenic injections and for knock-ins in zebrafish (*54*–*57*). PCR-based genotyping for the genomic *attP* integration or *attP*/*attB* recombination as well as germline segregation patterns of these transgenic insertions confirmed their nontargeted integration (see Supplementary Methods). Similar integrations have been well-documented in mice when targeting the *attP* sites in the *H11* locus, documenting background integrations as a universal caveat of vector-based transgene injections (*18*, *21*). Nonetheless, our genotyping PCR to verify proper transgene integration into *attP* landing sites (together with careful screening via fluorescence microscopy for fluorescent reporter-carrying transgenes) enables selection of correctly targeted transgenes into the *pIGLET14a* and *pIGLET24b* landing sites. All F1 animals with the expected targeted transgene integration (across and within F0 clutches) should exhibit uniform transgene expression. With fluorescent reporters, aberrant integrations can be identified in clutches that show mixed expression levels or patterns of the desired transgenic reporter pattern (*22*).

Functional testing of enhancers using *pIGLET* landing sites

Targeted transgenesis into a known and robust genomic location opens the possibility of qualitative and quantitative reporter comparisons of gene regulatory elements between wild type and variants such as polymorphisms, transcription factor (TF) binding site deletions, etc. (applications which have remained challenging with random transgenesis). We first sought to validate this approach using *pIGLET* by testing TF binding site deletion in the autoregulatory *Hs_I* notochord enhancer of the human *Brachyury*/*TBXT* gene that drives reporter activity in the notochord of zebrafish, axolotl, and mice (Fig. 4, A and B) (*58*). Removal of a Tbox motif in *Hs_I* results in loss of reporter expression in F0-injected zebrafish using *Tol2*-transgenesis constructs (*58*). To recapitulate this result using the *pIGLET* system, we cloned the wild type and the Tbox deletion variant of enhancer *Hs_I* into *attB* site–carrying reporter vectors (*Hs_I:min-mCerulean,exorh:EGFP* and *Hs_IΔTbox:min-mCerulean,exorh:EGFP*) (Fig. 4, B to D). To compare F0 notochord reporter mosaicism between *pIGLET* and *Tol2*-based transgenesis, we injected *Hs_I:min-mCerulean,exorh:EGFP* into *pIGLET14a* homozygous embryos and *Tol2*-based *Hs_I:min-mApple,exorh:EGFP* (*58*) into wild-type embryos in parallel and scored F0 expression based on percentage of notochord fluorescence coverage (Fig. 4, B to E, and fig S6, A and B). Injection of the Tbox deletion variant *Hs_IΔTbox:min-mCerulean,exorh:EGFP* into *pIGLET14a* resulted in complete loss of notochord expression, consistent with previous *Tol2*-based F0 results (Fig. 4D) (*58*). Although both transgenesis methods achieved F0 embryos with 80 to 100% fluorescent coverage across notochords for the wild-type *Hs_I* reporters (Fig. 4, B, C, and E), *pIGLET*-based injections yielded a significantly higher percentage of nearly complete notochord reporter activity among injected embryos (*Tol2:* 4.72% versus *pIGLET*: 27.42%) (Fig. 4E). This result documents lower F0 mosaicism using the *pIGLET* system compared to *Tol2* and is consistent with our observations of F0 expression following injection of *drl:EGFP* and *lmo2:EGFP* constructs into homozygous landing site embryos (90 to 95% transgene positive in injected clutches, approximately 25% displaying strong expression) (fig. S7, A to H). Indicative of early genomic integration after injection, this additional feature of our two *pIGLET* lines potentially facilitates selection and screening of regulatory elements for subsequent germline transmission.

We next sought to validate *pIGLET*-based enhancer testing with a human disease-associated, noncoding variant. Enhancer (*enh9B*) within the human *TBX5/TBX3* gene cluster has previously been described to harbor a single-nucleotide polymorphism (SNP) ($T > G$) that associates with congenital heart defects (Fig. 4F) (*59*). In stable transgenic reporter mice, *enh9* drives reporter expression in the cardiac ventricles and more broadly throughout the embryo in regions associated with both *TBX5* and *TBX3* activity, while zebrafish reporter expression was only reported for injection-based F0 assays (*59*). Stable mouse reporter transgenes for the SNP ($T > G$) showed greatly reduced or lost cardiac reporter activity, with uncharacterized impact on other expression domains (*59*). After generating *attB*-based transgenesis vectors for *Hs_enh9B*^{wt} from wild-type reference and *Hs_enh9B*$^{T>G}$ from variant sequences for zebrafish transgenesis using *pIGLET*, we isolated stable targeted integrations for each in *pIGLET14a* (Fig. 4, G and H). Consistent with *TBX3* expression in diverse ganglion populations in zebrafish and mice (*60*–*63*), we observed prominent reporter activity of *Hs_enh9B*^{wt}*:min-mCherry* in ventral anterior lateral line ganglia (Fig. 4G). In contrast, integrated at the same locus, the SNP version *Hs_enh9B*$^{T>G}$*:min-mCherry* showed loss of activity in these ganglia (Fig. 4H). In either line, we did not observe any cardiac reporter expression, arguing against a conserved activity of this enhancer in the heart. Together, these results show the utility of *pIGLET*-based transgenesis in zebrafish to qualitatively assess regulatory element activity of variants associated with human disease.

DISCUSSION

phiC31 integrase–mediated transgenesis into well-established landing sites has been transformative for work in *Drosophila* and mice (*18*–*21*). Our proof-of-concept experiments here establish the *attP* landing sites *pIGLET14a* and *pIGLET24b* for highly efficient, reproducible, and quality-controllable transgenesis using phiC31 integrase in zebrafish. We consistently observed that our *pIGLET*-based targeted, single-integration reporter transgenes show uniform and consistent activity across clutches and generations, hallmarks of high-quality transgenics (fig. S8). Our protocols outlined here pave the way to expand the repertoire of validated landing sites available to the model and enable critical transgene-based techniques.

Transgenesis into established *attP* landing sites in *Drosophila* and mouse hinged on identifying suitable sites by screening and validation of random integrations (*18*–*21*). Our data here indicate that *attP*-based landing sites with favorable properties can be generated in zebrafish by repurposing well-validated transgenes that have remained functional for numerous generations. Our approach is particularly suitable to convert existing *Tol2*-based transgenes with matching guide RNAs (fig. S1). The original *Tol2*-based *ubi:Switch* integration dates back to 2009 (*17*, *29*), and *hsp70l:Switch* was isolated in 2016 (*17*, *28*), with *ubi:Switch* in use with numerous zebrafish labs since distribution started in 2010. CRISPR-Cas9–mediated conversion of *Tol2*-based transgenes to *attP* landing sites via a two-step process (or one-step if the native locus is amenable) is applicable to other well-established transgenes available in the field and potentially any other model system.

Our demonstration of predictable, standardized, highly efficient transgene integration and suitability to generate previously challenging reporters such as *loxP* Switches establishes *pIGLET14a* and *pIGLET24b*

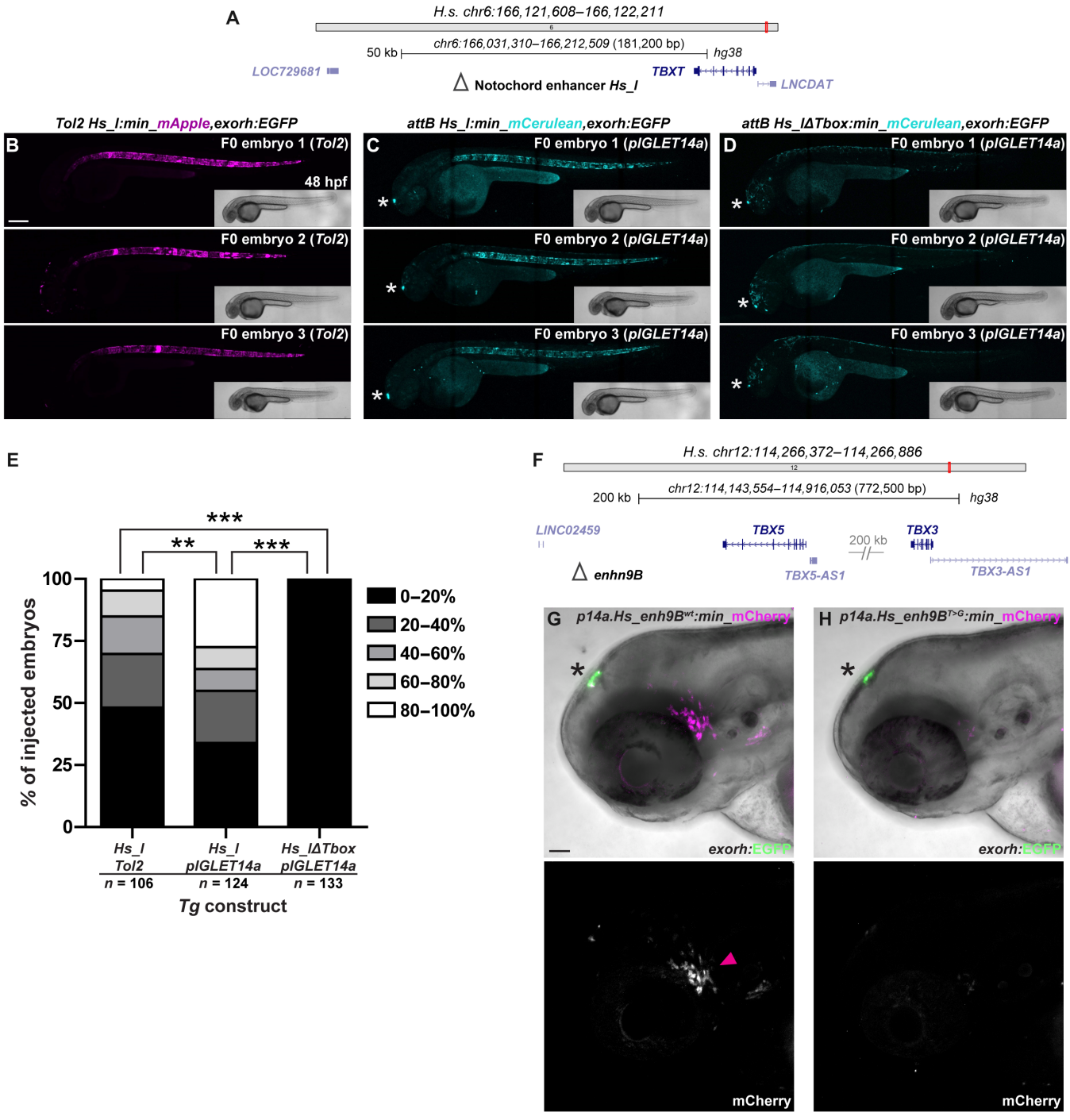

Fig. 4. *pIGLET*-based transgenesis facilitates reproducible enhancer variant testing in Zebrafish. (**A** to **E**) F0 injection–based testing of notochord enhancer *Hs_I* using *Tol2*- and *pIGLET*-based transgenesis. Schematic of *TBXT* locus with *Hs_I* annotated (A). Confocal imaging for mApple (B) or mCerulean (C and D) with bright-field inserts, anterior to the left. Both *Tol2*- and *pIGLET14a*-based F0 injections of *Hs_I:min-mApple/mCerulean,exorh;EGFP* result in embryos showing reporter expression with 80 to 100% fluorescent notochord coverage (B and C). Removal of the Tbox motif from *Hs_I* results in a complete loss of notochord reporter activity (D). Injected zebrafish are sorted for the *exorh:EGFP* transgenesis marker (white asterisk) to confirm successful injection (C and D). *pIGLET14a*-based F0 injections of *Hs_I:min-mCerulean,exorh:EGFP* show significantly more embryos with 80 to 100% fluorescent notochord coverage compared to *Tol2*-based injections and the Tbox motif deletion variant (E). (**F** to **H**) Comparison of stable reporter lines driven by the human *TBX5/TBX3*-associated enhancer *9B* (*Hs_enh9B*, *wt* versus *T* > *G* variant). Schematic of *TBX5/3* locus with *enh9B* annotated (F). *Hs_enh9B*^{wt} drives reporter expression in the ventral lateral line ganglia (magenta arrowhead) (G). Compared to *wt*, the disease-associated variant *Hs_enh9B*$^{T>G}$ exhibits nearly a complete loss of *mCherry* reporter expression (G and H). F1 heterozygous embryos are depicted (G and H). Scale bars: 200 μm (B) and 50 μm (G).

as widely applicable reagents for zebrafish transgenesis. Our provided protocols and recommended quality control steps use standard reagents and workflows established for general zebrafish transgenesis, supporting simple implementation (see also Materials and Methods and Supplementary Methods). Complementing existing random transgenesis performed with prior methods in the field (Tol2 and I-SceI), our first *pIGLET* landing sites enable streamlined transgenic strain generation with reduced screening and animal numbers. Targeted, reproducible transgene integration into validated sites proposes the use of *pIGLET* for large-scale transgene tests with quantitative and qualitative readouts in zebrafish applicable to disease variant testing, mechanistic investigation of gene regulatory elements, and more.

Being homozygous viable, our first two landing sites enable combinatorial use of maximally four individual transgenes. Future efforts to establish additional *pIGLET* landing site lines will greatly expand the possibilities for combinatorial transgene experiments and choice of tailored landing sites for specific transgene applications (*22*, *26*, *27*). Strategic generation and validation of additional *pIGLET* landing sites have the potential to enable methods involving controlled mitotic chromosome arm recombination such as the Mosaic Analysis with a Repressible Cell Marker (*64*) or Mosaic Analysis with Double Markers (*65*) systems applied in *Drosophila* and mice, respectively, for next-level cell labeling and conditional loss-of-function experiments. Given access to the same *pIGLET* lines, transgenic strains can be reproduced in different labs by mere sharing of the original transgenesis vector, which has the potential to drastically expand opportunities for worldwide reagent sharing in the field.

MATERIALS AND METHODS

Landing site creation (two-step)

Step 1: ubi:Switch and hsp70l:Switch transgene deletion

sgRNAs targeting *Tol2* arms (*Tol2 ccA* and *Tol2 ccB*) were coinjected with a ssODN containing the 84-bp *attP1* sequence and symmetric homology arms (48 bp) into *ubi:Switch* or *hsp70l:Switch* homozygous embryos (Thermo Fisher Scientific, polyacrylamide gel electrophoresis–purified, sequence details below). Injected F0 zebrafish were raised and out-crossed to identify transgene-negative progeny, indicative of full or partial transgene deletion or *attP1* insertion. Transgene-negative progeny was PCR-assayed (primers: *oRL095 Tol2 remnant Fw* and *oRL096 Tol2 remnant Rev*) and sequenced to test for transgene deletion/*attP1* insertion, with the absence of any PCR product suggesting partial transgene retention. No injected zebrafish contained the *attP1* insertion. The 1/20 injected zebrafish for both the *ubi:Switch* and *hsp70l:Switch locus*, transmitted F1 progeny with perfect or near perfect (single SNP) transgene deletion between the *Tol2* sgRNA target sites. Single F1 transgene deletion zebrafish were then out-crossed, and heterozygous F2 zebrafish were in-crossed for the next step.

Step 2: attP1 landing site insertion

A single sgRNA targeting the *Tol2* arm remnants (*Tol2 ccC*) was coinjected with a ssODN (2.0, sequence details below) containing the 84-bp *attP1* sequence and asymmetric homology arms (37 and 59 bp) into F2 heterozygous in-crossed *ubi:Switch* or *hsp70l:Switch* transgene deletion animals. F0 zebrafish were raised, fin clipped, PCR-assayed (primers: *oRL095 Tol2 remnant Fw* and *oRL096 Tol2 remnant Rev*) and sequenced to test for evidence of *attP1* insertion. F0 zebrafish that displayed *attP1* sequence insertion in the somatic tissue (fin clip) invariantly transmitted the same alleles in the germ line, indicating that homology-directed repair occurred early during development. From zebrafish that contained the *Tol2* arm remnant target site, 1/18 showed an 81-bp *attP1* insertion at the *ubi:Switch* locus, and 1/35 showed an 80-bp *attP1* insertion at the *hsp70l:Switch* locus. Single F1 heterozygous zebrafish (now termed *pIGLET14a* and *pIGLET24b*) were out-crossed, and heterozygous F2 zebrafish were in-crossed to obtain F3 homozygous *pIGLET14a* and *pIGLET24b* zebrafish.

Landing site nomenclature

Following discussions with users in the field and current transgene nomenclature (*66*), we included chromosome numbers and letter designation to distinguish future landing sites on the same chromosomes (*pIGLET14a*, *pIGLET14b*, *pIGLET14c*, etc.). We highly encourage the next landing site generated on chromosome 24 to take the *pIGLET24a* designation. Because of the timing of reagent sharing before publication and previous internal line designations, we kept the nomenclature for the first two landing site lines as *pIGLET14a* and *pIGLET24b*.

ZFIN line designations

ZFIN line designations are as follows: *pIGLET14a = co2001*; *pIGLET24b = co2002*; *p14a:drl:EGFP = co2003*; *p24b:drl:EGFP = co2004*;*p14a.lmo2:EGFP,cryaa:Venus=co2005*;*p24b.lmo2:EGFP,cryaa:Venus = co2006*; *p14a.elavl3:mCherry,exorh:EGFP = co2007*; *p24b.elavl3:mCherry,exorh:EGFP = co2008*; *p14a.drl:creERT2,cryaa:Venus = co2009*; *p24b.drl:creERT2,cryaa:Venus = co2010*; *p14a.hsp70l:Switch2,cryaa:Venus = co2011*; *p24b.hsp70l:Switch2,cryaa:Venus = co2012*; *p14a.Hs_enh9B^{wt}:mCherry,exorh:EGFP = co2013*; *p14a.Hs_enh9B$^{T>G}$:mCherry,exorh:EGFP = co2014*.

RNP complex preparation

Injection mixes for both step 1 and step 2 were made as per our previous work (*30*) using the following final concentrations: Cas9 (0.8 μg/μl; Alt-R S.p. Cas9 Nuclease V3, 100 μg; IDT, #1081058), ssODN (60 ng/μl), 0.05% phenol red, and 300 mM KCl, make up the total volume with sgRNA.

sgRNA target sites

sgRNA target sites are as follows: *Tol2 ccA:* 5′-GGGCATCAGCGCAATTCAAT-3′; *Tol2 ccB*: 5′-GTGTATTAGTCTTGATAGAG-3′; *Tol2 ccC*: 5′-AGTGCTGAAAAGCCTCTCAC-3′.

ssODN sequences

ssODN sequences are as follows: *attP1* (bold/underlined) ssODN: 5′-TTTGGAGATCACTTCATTCTATTTTCCCTTGCTATTACCAAACCAATT**AGAAGCGGTTTTCGGGAGTAGTGCCCCAACTGGGGTAACCTTTGAGTTCTCTCAGTTGGGGGCGTAGGGTCGCCGACATGACAC**TATCAAGACTAATACACCTCTTCCCGCATCGGCTGCCTGTGAGAGGCT-3′; *attP1* (bold/underlined) ssODN 2.0: 5′-ATCAAGACTAATACACCTCTTCCCGCATCGGCTGCCT**AGAAGCGGTTTTCGGGAGTAGTGCCCCAACTGGGGTAACCTTTGAGTTCTCTCAGTTGGGGGCGTAGGGTCGCCGACATGACAC**GTGAGAGGCTTTTTCAGCACTGCAGGATTGCTTTTCAGCCCCAAAAGAGCTAGGCTTGAC-3′.

Primer sequences

Primer sequences are as follows: *oRL095 Tol2 remnant Fw*: 5′-ATTGCCAGAGGTGTAAAGTA-3′; *oRL096 Tol2 remnant Rev*: 5′-CCAGTACACGCTACTCAAA-3′.

pIGLET14a and pIGLET24b genotyping

Unrecombined, native *attP1* alleles: *oRL095 Tol2 remnant Fw* + *oRL096 Tol2 remnant Rev* (the expected size is ~500 to 520 bp, depending on *pIGLET14a* or *pIGLET24b*). PCR program is as follows: 30 cycles, melting temperature (Tm) = 54°C, and extension = 30 s.

pIGLET14a$^{+/+}$ or *pIGLET14a*$^{-/+}$ genotyping: *oRL168 ubi:Switch locus Fw* + *oRL169 ubi:Switch locus Rev* (the expected size is 1448 bp for the presence of landing site and 623 bp for the absence of landing site). PCR program is as follows: 30 cycles, Tm = 65°C, and extension = 1 min *oRL168 ubi:Switch locus Fw: 5′-CATGATCGAAAACGAGCAATGTC-3′* and *oRL169 ubi:Switch locus Rev*: *5′-GACTGCGTCACTTTGACAACCCTG-3′*.

pIGLET24b$^{+/+}$ or *pIGLET24b*$^{-/+}$ genotyping: *oRL074 hsp70l:Switch locus Fw* + *oRL073 hsp70l:Switch locus Rev* (the expected size is 1421 bp for the presence of landing site and 619 bp for the absence of landing site). PCR program is as follows: 30 cycles, Tm = 57°C, and extension = 1 min; *oRL074 hsp70l:Switch locus Fw*: *5′-GCATGACACGGCTAACCAAC-3′* and *oRL073 hsp70l:Switch locus Rev*: *5′-TATCAGCACACACCTTTATCGC-3′*.

Transgenic line creation

Single-cell *pIGLET14a* and *pIGLET24b* embryos were coinjected with expression plasmid (25 ng/μl; containing phiC31-recognized–compatible *attB* recombination cassette) and phiC31 *integrase* mRNA (25 ng/μl). Ten to 20 F0 embryos/construct were euthanized to check for targeted integration as described in the Supplementary Methods (printable for bench use). A total of ~25 to 50 % of transmitted F1 embryos from the first transgene-positive clutch were genotyped to check for correct integration. Only clutches that showed 100% targeted integration were raised. F1 adults were genotyped by fin clip to check for targeted integration and out-crossed to check for expected Mendelian transmission ratios in the next generation (50% transgene positive), indicative of single-copy transgene insertions.

For detailed integration methods, including sample gels and quality control suggestions, and steps to create DNA sequence map of plasmid integrations into *pIGLET14a* and *pIGLET24b* loci, please see Supplementary Methods. Of note, if *pRL092 pattB_cryaa:Venus_MCS* or *pRL093 pattB_exorh:EGFP_MCS* were used for expression plasmid construction, then a customized *Fw* primer will be needed in place of primer *attB2 Fw* to sequence-confirm the cloned 3′ integration boundary.

phiC31 integrase mRNA

pCDNA3.1 phiC31 integrase (Addgene, #68310) (*20*, *22*) plasmid was linearized with Bam HI and transcribed using the T7 mMessage mMachine kit (Thermo Fisher Scientific, AM1344). Following in vitro transcription (IVT), mRNA was treated with Turbo deoxyribonuclease (DNase) cleaned using LiCl precipitation methods as described in the T7 mMessage mMachine kit protocol. Briefly, following Turbo DNAse treatment, 30 μl of nuclease-free water and 30 μl of LiCl were added, and the reaction was precipitated overnight at −20°C. Following a 15-min maximum speed centrifugation, 750 μl of cold 70% ethanol (EtOH) was added, and the reaction was spun again for 10 min at maximum speed. After careful removal of EtOH, the pellet was air-dried and resuspended in 20 μl of nuclease-free water. Clean preps of phiC31 *integrase* mRNA are well-tolerated by zebrafish embryos; if excessive mortality is observed, then IVT of a fresh mRNA batch and careful cleanup are recommended.

4-OHT inductions and heat shock treatments

Activity of CreERT2 was induced with 10 μM final concentration of 4-OHT (Sigma-Aldrich, St. Louis, Missouri, H7904, abbreviated as 4-OHT) in E3 (*67*). 4-OHT stock is stored at −20°C in the dark as 10 mM single-use aliquots dissolved in dimethyl sulfoxide and used within 2 months of dissolving. Before administration, the 4-OHT aliquots were incubated at 65°C for 10 min and vortexed (*67*). For shield stage treatment, 4-OHT was administered overnight and then replaced with *N*-phenylthiourea (PTU; Sigma-Aldrich, P7629) at a final concentration of 150 μM in E3 embryo medium each morning to inhibit melanogenesis.

To trigger fluorophore expression, *hsp70l:Switch* and *p14a/p24b. hsp70l:Switch2* embryos were heat-shocked for 1 hour at 37°C in a dedicated water bath. Before heat shock, embryos were dechorionated and transferred to a glass vial with E3 medium. Embryos were imaged 3 to 4 hours (confocal microscope) later.

Genomic DNA isolation

To isolate genomic DNA, embryos/fin clips are sorted into 0.2-μl PCR tubes containing 50 μl of 50 mM NaOH solution. Using a thermocycler, tubes are then heated for 20 min at 95°C and then cooled to 12°C. Afterward, 5 μl of 1.0 M Tris buffer (pH 8.0) is added, and genomic preps are stored at 4°C. One to 2 μl is used for a typical PCR reaction.

Plasmid construction

All plasmids were created with the Multisite Gateway system with LR Clonase II Plus (Life Technologies, catalog no. 12538120) according to the manufacturer's instructions and original Tol2 Kit information (*2*, *31*), assemblies were described below, and vector ratios were calculated using the Multisite Gateway Excel Spreadsheet (*68*):

pCM318 drl:EGFP: *pCM293 pENTR5′*_6.3-kb *drl* regulatory region (*32*), *#383 pENTR/D_EGFP* (*2*), *#302 p3′_SV40 polyA* (*2*), and *pCM268 pDESTattB* (*22*) (Addgene, #68313).

pCM328 lmo2:EGFP,cryaa:Venus: *pENTR5′_lmo2* upstream region (*36*), *#383 pENTR/D_EGFP* (*2*), #302 *p3′_SV40 polyA* (*2*), and *pCM327 pDESTattB_cryaa:Venus* (*22*) (Addgene, #68341).

pRL058 elavl3:mCherry,exorh:EGFP: *pENTR5′*_8.7-kb *elavl3* (*HuC*) (*38*), #456 *pENTR/D*_mCherry (*2*), *pGD003 p3′_ubbpA* (*31*), and *pRL056 pDESTattB_exorh:EGFP.*

*pRL045 drl:creERT2,cryaa:Venus: pCM293 pENTR5′*_6.3-kb *drl* regulatory region (*32*), *pENTR/D_creERT2* (Addgene, #27321) (*29*), *pGD003 p3'_ubbpA* (*31*), and *pRL055 pDESTattB_cryaa:Venus.*

pRL069hsp70l:Switch2,cryaa:Venus:pDH083pENTR5′_hsp70l:loxP-Stop-loxP (*69*), *#763 pENTR/D_mApple* (*31*), *pGD003 p3′_ubbpA* (*31*), and *pRL055 pDESTattB_cryaa:Venus.*

pRL050 Hs_enh9B^{wt}*:min-mCherry,exorh:EGFP*: *pRL049 pENTR5′_Hs_enh9B*^{wt}, *pCK006 pENTR/D_min-mCherry* (*31*), *pGD003 p3′_ubbpA* (*31*), and *pRL056 pDESTattB_exorh:EGFP.*

pRL052 Hs_enh9B$^{T>G}$*:min-mCherry, exorh:EGFP*: *pRL051 pENTR5′_Hs_enh9*$^{T>G}$, *pCK006 pENTR/D_min-mCherry* (*31*), *pGD003 p3′_ubbpA* (*31*), and *pRL056 pDESTattB_exorh:EGFP.*

pCK086 Hs_I:min-mCerulean, exorh:EGFP: *pENTR5′_Hs_I* (*58*), *pSN001 pENTR/D_min-mCerulean* (*31*), #302 *p3′_SV40 polyA* (*2*), and *pRL056 pDESTattB_exorh:EGFP.*

pCK085 Hs_IdelTbox:min-mCerulean, exorh:EGFP: *pCK075 pENTR5′_Hs_IdelTbox* (*58*), *pSN001 pENTR/D_min-mCerulean* (*31*), #302 *p3′_SV40 polyA* (*2*), and *pRL056 pDESTattB_exorh:EGFP.*

pENTR5′ pRL049 Hs_enh9B^{wt} and *pENTR5′ pRL051 Hs_enh9B$^{T>G}$* cloning

pRL049 Hs_enh9B^{wt} was amplified with the following primers, using human genomic DNA as template, and then cloned into the *pENTR5′-TOPO* vector (Thermo Fisher Scientific, #K59120): *oRL163 Hs_enh9B Fw*: *5′-AGTAGGGGGATGCTAATTTCATAGC-3′*; *oRL164 Hs_enh9B Rev*: *5′-TCTCAAGTCCTCTTGCGGTTTTGA-3′*. *pRL051 Hs_enh9$^{T>G}$* was cloned using *pRL049* as a template for overlapping PCR to introduce the *T* > *G* mutation at base pair position 339 using the following primers: *oRL165 Hs_enh9B overlap Rev: 5′-CCCAACAGTTTCCAAGCATATTGAATATATTGTGGTCAG-3′*; *oRL166 Hs_enh9B overlap Fw: 5′-CTGACCACAATATATTCCATATTCTTGGAAACTGTTGGG-3′*.

The products of *oRL163 Fw* + *oRL65 Rev* and *oRL166 Fw* + *oRL164 Rev* were individually column-purified, and 1 μl of each was combined as template for a final PCR reaction using *oRL163 Fw* + *oRL164 Rev*. The final product was then cloned into the *pENTR5′-TOPO* vector (Thermo Fisher Scientific, #K59120).

Imaging

PTU-treated (150 μM) embryos were anesthetized at 10 ss for 2 days postfertilization with 0.016 % Tricaine-S (MS-222, Pentair Aquatic Ecosystems, Apopka, Florida, NC0342409) in E3 embryo medium. Standard fluorescence imaging was performed on a Leica M205FA with a DFC450 C camera. Laser scanning confocal microscopy was performed on a Zeiss LSM880 following embedding in E3 with 1 % low–melting point agarose (Sigma-Aldrich, A9045) on glass-bottom culture dishes (Greiner Bio-One, Kremsmunster, Austria, 627861). Images were collected with a ×10/0.8 and ×20/0.8 air-objective lens with all channels captured sequentially with maximum speed in bidirectional mode, with the range of detection adjusted to avoid overlap between channels. Maximum projections of acquired Z-stacks were made using ImageJ/Fiji and cropped and rotated using Adobe Photoshop.

Statistics

For Fig. 3D, each category of notochord fluorescent coverage was scored between 1 and 5 (0 to 20% = 1, 20 to 40% = 2, 40 to 60% = 3, 60 to 80% = 4, 80 to 100% = 5), and the sum/average of the fluorescent coverage scores per group was calculated. The average fluorescent coverage score of each group was then compared to each other using Kruskal-Wallis test with Dunn's correction for multiple tests. The proportion of embryos presenting each fluorescent coverage score per group is included. Adjusted *P* values after multiple tests correction are reported, and significance was set at $P < 0.0001$. GraphPad Prism 9.0.2 was used to perform statistical tests and generate graphs.

Supplementary Materials

This PDF file includes:
Supplementary Methods
Figs. S1 to S8
Tables S1 and S2
Legend for data file S1

Other Supplementary Material for this manuscript includes the following:
Data file S1

REFERENCES AND NOTES

1. A. Felker, C. Mosimann, Contemporary zebrafish transgenesis with Tol2 and application for Cre/lox recombination experiments. *Methods Cell Biol.* **135**, 219–244 (2016).
2. K. M. Kwan, E. Fujimoto, C. Grabher, B. D. Mangum, M. E. Hardy, D. S. Campbell, J. M. Parant, H. J. Yost, J. P. Kanki, C. Bin Chien, The Tol2kit: A multisite gateway-based construction kit for Tol2 transposon transgenesis constructs. *Dev. Dyn.* **236**, 3088–3099 (2007).
3. H. Kikuta, K. Kawakami, Transient and stable transgenesis using tol2 transposon vectors. *Methods Mol. Biol.* **546**, 69–84 (2009).
4. T. J. Carney, C. Mosimann, Switch and trace: Recombinase genetics in zebrafish. *Trends Genet.* **34**, 362–378 (2018).
5. K. Kawakami, Tol2: A versatile gene transfer vector in vertebrates. *Genome Biol.* **8**, 1–10 (2007).
6. K. Kawakami, K. Asakawa, A. Muto, H. Wada, Tol2-mediated transgenesis, gene trapping, enhancer trapping, and Gal4-UAS system. *Methods Cell Biol.* **135**, 19–37 (2016).
7. V. Thermes, C. Grabher, F. Ristoratore, F. Bourrat, A. Choulika, J. Wittbrodt, J. S. Joly, I-SceI meganuclease mediates highly efficient transgenesis in fish. *Mech. Dev.* **118**, 91–98 (2002).
8. D. Soroldoni, B. M. Hogan, A. C. Oates, Simple and efficient transgenesis with meganuclease constructs in zebrafish. *Methods Mol. Biol.* **546**, 117–130 (2009).
9. S. Albadri, F. Del Bene, C. Revenu, Genome editing using CRISPR/Cas9-based knock-in approaches in zebrafish. *Methods* **121-122**, 77–85 (2017).
10. G. Kesavan, J. Hammer, S. Hans, M. Brand, Targeted knock-in of CreER T2 in zebrafish using CRISPR/Cas9. *Cell Tissue Res.* **372**, 41–50 (2018).
11. E. de Vrieze, S. E. de Bruijn, J. Reurink, S. Broekman, V. van de Riet, M. Aben, H. Kremer, E. van Wijk, Efficient generation of knock-in zebrafish models for inherited disorders using CRISPR-Cas9 ribonucleoprotein complexes. *Int. J. Mol. Sci.* **22**, (2021).
12. H. M. Thorpe, S. E. Wilson, M. C. M. Smith, Control of directionality in the site-specific recombination system of the Streptomyces phage phiC31. *Mol. Microbiol.* **38**, 232–241 (2000).
13. H. M. Thorpe, M. C. M. Smith, In vitro site-specific integration of bacteriophage DNA catalyzed by a recombinase of the resolvase/invertase family. *Proc. Natl. Acad. Sci. U.S.A.* **95**, 5505–5510 (1998).
14. B. G. Allen, D. L. Weeks, Bacteriophage phiC31 integrase mediated transgenesis in Xenopus laevis for protein expression at endogenous levels. *Methods Mol. Biol.* **518**, 113–122 (2009).
15. E. Sangiorgi, Z. Shuhua, M. R. Capecchi, In vivo evaluation of PhiC31 recombinase activity using a self-excision cassette. *Nucleic Acids Res.* **36**, –e134 (2008).
16. S. Pellenz, M. Phelps, W. Tang, B. T. Hovde, R. B. Sinit, W. Fu, H. Li, E. Chen, R. J. Monnat, New human chromosomal sites with "safe harbor" potential for targeted transgene insertion. *Hum. Gene Ther.* **30**, 814 (2019).
17. R. L. Lalonde, C. L. Kemmler, F. W. Riemslagh, A. J. Aman, J. Kresoja-Rakic, H. R. Moran, S. Nieuwenhuize, D. M. Parichy, A. Burger, C. Mosimann, Heterogeneity and genomic loci of ubiquitous transgenic Cre reporter lines in zebrafish. *Dev. Dyn.* **251**, 1754–1773 (2022).
18. B. Tasic, S. Hippenmeyer, C. Wang, M. Gamboa, H. Zong, Y. Chen-Tsai, L. Luo, Site-specific integrase-mediated transgenesis in mice via pronuclear injection. *Proc. Natl. Acad. Sci. U.S.A.* **108**, 7902–7907 (2011).
19. J. M. Knapp, P. Chung, J. H. Simpson, Generating customized transgene landing sites and multi-transgene arrays in Drosophila using phiC31 integrase. *Genetics* **199**, 919–934 (2015).
20. J. Bischof, R. K. Maeda, M. Hediger, F. Karch, K. Basler, An optimized transgenesis system for Drosophila using germ-line-specific φC31 integrases. *Proc. Natl. Acad. Sci. U.S.A.* **104**, 3312–3317 (2007).
21. C.-m. Chen, J. Krohn, S. Bhattacharya, B. Davies, A comparison of exogenous promoter activity at the ROSA26 locus using a PhiC31 integrase mediated cassette exchange approach in mouse ES cells. *PLOS ONE* **6**, e23376 (2011).
22. C. Mosimann, A.-C. Puller, K. L. Lawson, P. Tschopp, A. Amsterdam, L. I. Zon, Site-directed zebrafish transgenesis into single landing sites with the phiC31 integrase system. *Dev. Dyn.* **242**, 949–963 (2013).
23. J. A. Lister, Transgene excision in zebrafish using the phiC31 integrase. *Genesis* **48**, 137–143 (2010).
24. G. Hu, M. G. Goll, S. Fisher, ΦC31 integrase mediates efficient cassette exchange in the zebrafish germline. *Dev. Dyn.* **240**, 2101–2107 (2011).
25. S. Kirchmaier, B. Höckendorf, E. K. Möller, D. Bornhorst, F. Spitz, J. Wittbrodt, Efficient site-specific transgenesis and enhancer activity tests in medaka using PhiC31 integrase. *Development* **140**, 4287–4295 (2013).
26. J. A. Roberts, I. Miguel-Escalada, K. J. Slovik, K. T. Walsh, Y. Hadzhiev, R. Sanges, E. Stupka, E. K. Marsh, J. Balciuniene, D. Balciunas, F. Müller, Targeted transgene integration overcomes variability of position effects in zebrafish. *Development* **141**, 715–724 (2014).
27. S. Bhatia, D. J. Kleinjan, K. Uttley, A. Mann, N. Dellepiane, W. A. Bickmore, Quantitative spatial and temporal assessment of regulatory element activity in zebrafish. *eLife* **10**, e65601 (2021).

28. A. Felker, K. D. Prummel, A. M. Merks, M. Mickoleit, E. C. Brombacher, J. Huisken, D. Panáková, C. Mosimann, Continuous addition of progenitors forms the cardiac ventricle in zebrafish. *Nat. Commun.* **9**, 1–14 (2018).
29. C. Mosimann, C. K. Kaufman, P. Li, E. K. Pugach, O. J. Tamplin, L. I. Zon, Ubiquitous transgene expression and Cre-based recombination driven by the ubiquitin promoter in zebrafish. *Development* **138**, 169 (2011).
30. A. Burger, H. Lindsay, A. Felker, C. Hess, C. Anders, E. Chiavacci, J. Zaugg, L. M. Weber, R. Catena, M. Jinek, M. D. Robinson, C. Mosimann, Maximizing mutagenesis with solubilized CRISPR-Cas9 ribonucleoprotein complexes. *Development* **143**, 2025–2037 (2016).
31. C. L. Kemmler, H. R. Moran, B. F. Murray, A. Scoresby, J. R. Klem, R. L. Eckert, E. Lepovsky, S. Bertho, S. Nieuwenhuize, S. Burger, C. Betz, A.-C. Puller, A. Felker, K. Ditrychova, S. Bo, M. Affolter, N. Rohner, C. Ben Lovely, K. M. Kwan, A. Burger, C. Mosimann, Next-generation plasmids for transgenesis in zebrafish and beyond. *Development* **150**, dev201531 (2023).
32. C. Mosimann, D. Panáková, A. A. Werdich, G. Musso, A. Burger, K. L. Lawson, L. A. Carr, K. R. Nevis, M. K. Sabeh, Y. Zhou, A. J. Davidson, A. Dibiase, C. E. Burns, C. G. Burns, C. A. Macrae, L. I. Zon, Chamber identity programs drive early functional partitioning of the heart. *Nat. Commun.* **6**, 1–10 (2015).
33. K. D. Prummel, C. Hess, S. Nieuwenhuize, H. J. Parker, K. W. Rogers, I. Kozmikova, C. Racioppi, E. C. Brombacher, A. Czarkwiani, D. Knapp, S. Burger, E. Chiavacci, G. Shah, A. Burger, J. Huisken, M. H. Yun, L. Christiaen, Z. Kozmik, P. Müller, M. Bronner, R. Krumlauf, C. Mosimann, A conserved regulatory program initiates lateral plate mesoderm emergence across chordates. *Nat. Commun.* **10**, 3857 (2019).
34. K. D. Prummel, H. L. Crowell, S. Nieuwenhuize, E. C. Brombacher, S. Daetwyler, C. Soneson, J. Kresoja-Rakic, A. Kocere, M. Ronner, A. Ernst, Z. Labbaf, D. E. Clouthier, A. B. Firulli, H. Sánchez-Iranzo, S. R. Naganathan, R. O'Rourke, E. Raz, N. Mercader, A. Burger, E. Felley-Bosco, J. Huisken, M. D. Robinson, C. Mosimann, Hand2 delineates mesothelium progenitors and is reactivated in mesothelioma. *Nat. Commun.* **13**, 1677 (2022).
35. H. Zhu, D. Traver, A. J. Davidson, A. Dibiase, C. Thisse, B. Thisse, S. Nimer, L. I. Zon, Regulation of the lmo2 promoter during hematopoietic and vascular development in zebrafish. *Dev. Biol.* **281**, 256–269 (2005).
36. L. Wang, Y. Zhang, T. Zhou, Y. F. Fu, T. T. Du, Y. Jin, Y. Chen, C. G. Ren, X. L. Peng, M. Deng, X. L. Ting, Functional characterization of lmo2-Cre transgenic zebrafish. *Dev. Dyn.* **237**, 2139–2146 (2008).
37. C. H. Kim, E. Ueshima, O. Muraoka, H. Tanaka, S. Y. Yeo, T. L. Huh, N. Miki, Zebrafish elav/HuC homologue as a very early neuronal marker. *Neurosci. Lett.* **216**, 109–112 (1996).
38. T. Sato, M. Takahoko, H. Okamoto, HuC:Kaede, a useful tool to label neural morphologies in networks in vivo. *Genesis* **44**, 136–142 (2006).
39. H. C. Park, C. H. Kim, Y. K. Bae, S. Y. Yeo, S. H. Kim, S. K. Hong, J. Shin, K. W. Yoo, M. Hibi, T. Hirano, N. Miki, A. B. Chitnis, T. L. Huh, Analysis of upstream elements in the HuC promoter leads to the establishment of transgenic zebrafish with fluorescent neurons. *Dev. Biol.* **227**, 279–293 (2000).
40. A. A. Bianca Ulloa, S. S. Habbsa, K. S. Potts, M. Feliz Norberto, C. Mosimann, T. V. Bowman, Definitive hematopoietic stem cells minimally contribute to embryonic hematopoiesis. *Cell Rep.* **36**, 109703 (2021).
41. S. Sinha, M. M. Santoro, New models to study vascular mural cell embryonic origin: Implications in vascular diseases. *Cardiovasc. Res.* **114**, 481–491 (2018).
42. M. Hurskainen, I. Mižíková, D. P. Cook, N. Andersson, C. Cyr-Depauw, F. Lesage, E. Helle, L. Renesme, R. P. Jankov, M. Heikinheimo, B. C. Vanderhyden, B. Thébaud, Single cell transcriptomic analysis of murine lung development on hyperoxia-induced damage. *Nat. Commun.* **12**, 1–19 (2021).
43. K. C. Liu, A. Villasenor, M. Bertuzzi, N. Schmitner, N. Radros, L. Rautio, K. Mattonet, R. L. Matsuoka, S. Reischauer, D. Y. Stainier, O. Andersson, Insulin-producing b-cells regenerate ectopically from a mesodermal origin under the perturbation of hemato-endothelial specification. *eLife* **10**, (2021).
44. S. Hans, J. Kaslin, D. Freudenreich, M. Brand, Temporally-controlled site-specific recombination in zebrafish. *PLOS ONE* **4**, 4640 (2009).
45. M. A. McLellan, N. A. Rosenthal, A. R. Pinto, Cre-loxP-mediated recombination: General principles and experimental considerations. *Curr. Protoc. Mouse Biol.* **7**, 1–12 (2017).
46. I. Kobayashi, J. Kobayashi-Sun, A. D. Kim, C. Pouget, N. Fujita, T. Suda, D. Traver, Jam1a–Jam2a interactions regulate haematopoietic stem cell fate through Notch signalling. *Nature* **512**, 319–323 (2014).
47. J. Y. Bertrand, N. C. Chi, B. Santoso, S. Teng, D. Y. Stainier, D. Traver, Haematopoietic stem cells derive directly from aortic endothelium during development. *Nature* **464**, 108–111 (2010).
48. C. K. Kaufman, C. Mosimann, Z. P. Fan, S. Yang, A. J. Thomas, J. Ablain, J. L. Tan, R. D. Fogley, E. van Rooijen, E. J. Hagedorn, C. Ciarlo, R. M. White, D. A. Matos, A.-C. Puller, C. Santoriello, E. C. Liao, R. A. Young, L. I. Zon, A zebrafish melanoma model reveals emergence of neural crest identity during melanoma initiation. *Science* **351**, aad2197 (2016).
49. B. Hu, S. Lelek, B. Spanjaard, H. El-Sammak, M. G. Simões, J. Mintcheva, H. Aliee, R. Schäfer, A. M. Meyer, F. Theis, D. Y. R. Stainier, D. Panáková, J. P. Junker, Origin and function of activated fibroblast states during zebrafish heart regeneration. *Nat. Gene.* **54**, 1227–1237 (2022).
50. K. Mattonet, F. W. Riemslagh, S. Guenther, K. D. Prummel, G. Kesavan, S. Hans, I. Ebersberger, M. Brand, A. Burger, S. Reischauer, C. Mosimann, D. Y. R. Stainier, Endothelial versus pronephron fate decision is modulated by the transcription factors Cloche/Npas4l, Tal1, and Lmo2. *Sci. Adv.* **8**, 31 (2022).
51. A. L. Rubinstein, D. Lee, R. Luo, P. D. Henion, M. E. Halpern, Genes Dependent on Zebrafish cyclops Function Identified by AFLP Differential Gene Expression Screen. doi: 10.1002/(SICI)1526-968X(200001)26:1 (2000).
52. R. Luo, M. An, B. L. Arduini, P. D. Henion, Specific Pan-Neural Crest Expression of Zebrafish Crestin Throughout Embryonic Development. doi: 10.1002/1097-0177 (2001).
53. R. M. White, J. Cech, S. Ratanasirintrawoot, C. Y. Lin, P. B. Rahl, C. J. Burke, E. Langdon, M. L. Tomlinson, J. Mosher, C. Kaufman, F. Chen, H. K. Long, M. Kramer, S. Datta, D. Neuberg, S. Granter, R. A. Young, S. Morrison, G. N. Wheeler, L. I. Zon, DHODH modulates transcriptional elongation in the neural crest and melanoma. *Nature* **471**, 518–522 (2011).
54. R. Shankar, M. Schmeer, M. Schleef, Minicircles: Next-generation gene vectors. *Cell Gene. Ther. Insights* **3**, 285–300 (2017).
55. M. M. Munye, A. D. Tagalakis, J. L. Barnes, R. E. Brown, R. J. McAnulty, S. J. Howe, S. L. Hart, Minicircle DNA provides enhanced and prolonged transgene expression following airway gene transfer. *Sci. Rep.* **6**, 23125 (2016).
56. O. Argyros, S. P. Wong, C. Fedonidis, O. Tolmachov, S. N. Waddington, S. J. Howe, M. Niceta, C. Coutelle, R. P. Harbottle, Development of S/MAR minicircles for enhanced and persistent transgene expression in the mouse liver. *J. Mol. Med.* **89**, 515–529 (2011).
57. M. Keating, R. Hagle, D. Osorio-Méndez, A. Rodriguez-Parks, S. I. Almutawa, J. Kang, A robust knock-in approach using a minimal promoter and a minicircle. *Dev. Biol.* **505**, 24–33 (2024).
58. C. L. Kemmler, J. Smolikova, H. R. Moran, B. J. Mannion, D. Knapp, F. Lim, A. Czarkwiani, V. Hermosilla Aguayo, V. Rapp, O. E. Fitch, S. Bötschi, L. Selleri, E. Farley, I. Braasch, M. Yun, A. Visel, M. Osterwalder, C. Mosimann, Z. Kozmik, A. Burger, Conserved enhancers control notochord expression of vertebrate Brachyury. *Nat. Commun.* **14**, 6594 (2023).
59. S. Smemo, L. C. Campos, I. P. Moskowitz, J. E. Krieger, A. C. Pereira, M. A. Nobrega, Regulatory variation in a TBX5 enhancer leads to isolated congenital heart disease. *Hum. Mol. Genet.* **21**, 3255–3263 (2012).
60. I. Ribeiro, Y. Kawakami, D. Büscher, Á. Raya, J. Rodriguez-León, M. Morita, C. Rodríguez Esteban, J. C. Izpisúa Belmonte, Tbx2 and Tbx3 regulate the dynamics of cell proliferation during heart remodeling. *PLOS ONE* **2**, 398 (2007).
61. J. Andrew Gillis, K. E. Criswell, C. V H Baker, A. Gillis, C. Baker, The skate spiracular organ develops from a unique neurogenic placode, distinct from lateral line placodes. bioRxiv 2023.03.17.533203 [Preprint] (2023). doi: 10.1101/2023.03.17.533203.
62. C. V. H. Baker, P. O'Neill, R. B. Mccole, Lateral line, otic and epibranchial placodes: Developmental and evolutionary links? *J. Exp. Zool. B Mol. Dev. Evol.* **310**, 370 (2008).
63. A. S. Viczian, A. M. Moon, M. E. Zuber, A subset of retinal ganglion cells that control angiogenesis requires TBX3 for their formation. *Invest. Ophthalmol. Vis. Sci.* **64**, 3627–3627 (2023).
64. T. Lee, L. Luo, Mosaic analysis with a repressible cell marker for studies of gene function in neuronal morphogenesis. *Neuron* **22**, 451–461 (1999).
65. H. Zong, J. S. Espinosa, H. H. Su, M. D. Muzumdar, L. Luo, Mosaic analysis with double markers in mice. *Cell* **121**, 479–492 (2005).
66. Y. M. Bradford, C. E. Van Slyke, L. Ruzicka, A. Singer, A. Eagle, D. Fashena, D. G. Howe, K. Frazer, R. Martin, H. Paddock, C. Pich, S. Ramachandran, M. Westerfield, Zebrafish information network, the knowledgebase for Danio rerio research. *Genetics* **220**, iyac016 (2022).
67. A. Felker, S. Nieuwenhuize, A. Dolbois, K. Blazkova, C. Hess, L. W. L. Low, S. Burger, N. Samson, T. J. Carney, P. Bartunek, C. Nevado, C. Mosimann, In vivo performance and properties of tamoxifen metabolites for CreERT2 control. *PLOS ONE* **11**, e0152989 (2016).
68. C. Mosimann, Multisite Gateway Calculations: Excel spreadsheet. protocols.io [Preprint] (2022). https://doi.org/10.17504/protocols.io.b4xdqxi6.
69. D. Hesselson, R. M. Anderson, M. Beinat, D. Y. R. Stainier, Distinct populations of quiescent and proliferative pancreatic beta-cells identified by HOTcre mediated labeling. *Proc. Natl. Acad. Sci. U.S.A.* **106**, 14896–14901 (2009).

Acknowledgments: We thank C. Archer, A. Gilbard, and O. Gomez for zebrafish husbandry at CU Anschutz; all past and present members of the Mosimann lab for constructive input and support during the pursuit of this long-term project; Piglet the cat for acronym inspiration; and J. N. Acedo, M. C. Tobias, and A. Schier for critical input and field testing. **Funding:** This work was supported by Children's Hospital Colorado Foundation, The Helen and Arthur E. Johnson Chair for the Cardiac Research Director (C.M.), National Science Foundation Grant 2203311 (C.M.), NIH/NIDDK grant 1R01DK129350-01A1 (A.B.), SwissBridge Foundation (A.B. and C.M.), Additional Ventures SVRF2021-1048003 (A.B. and C.M.), University of Colorado Anschutz Medical Campus (A.B. and C.M.), NIH/NHLBI 1K99HL168148-01 (R.L.L.), and NIH/NIGMS

1T32GM141742-01 (H.H.W.). **Author contributions:** Conceptualization: R.L.L., S.N., C.M., and A.B. Methodology: R.L.L., H.H.W., C.L.K., S.N., R.L., A.B., and C.M. Investigation: R.L.L., H.H.W., C.L.K., S.N., R.L., A.B., and C.M. Visualization: R.L.L., H.H.W., S.N., and C.L.K. Funding acquisition: C.M. and A.B. Project administration: C.M. Supervision: C.M. and A.B. Writing—original draft: R.L.L. and C.M. Writing—review and editing: R.L.L., H.H.W., C.L.K., S.N., R.L., A.B., and C.M. **Competing interests:** The authors declare that they have no competing interests. **Data and materials availability:** All data needed to evaluate the conclusions in the paper are present in the paper and/or the Supplementary Materials. Zebrafish lines are being deposited with ZIRC (*pIGLET14a* as *co2001* and *pIGLET24b* as *co2002*), plasmid vectors are available at Addgene (https://addgene.org/browse/article/28243795/). Addgene plasmid accession numbers are the following: *pRL055 pDESTattB_cryaa:Venus* (#213509), *pRL056 pDESTattB_exorh:EGFP* (#213510), *pCK122 pDESTattB_exorh:mCherry* (#213511), *pCK123 pDESTattB_exorh:mCerulean* (#213512), *pRL092 pattB_cryaa:Venus_MCS* (#213513), and *pRL093 pattB_exorh:EGFP_MCS* (#213514).

Submitted 20 December 2023
Accepted 3 May 2024
Published 5 June 2024
10.1126/sciadv.adn6603